Video Article

Generation of a Chronic Obstructive Pulmonary Disease Model in Mice by Repeated Ozone Exposure

Zhongwei Sun[1,2], Feng Li[3], Xin Zhou[3], Wen Wang[1,2]

[1]Cellular Biomedicine Group, Shanghai

[2]Cellular Biomedicine Group, Cupertino

[3]Department of Respiratory Medicine, Shanghai General Hospital, Shanghai Jiaotong University

Correspondence to: Wen Wang at Maxwell.Wang@cellbiomedgroup.com

URL: https://www.jove.com/video/56095
DOI: doi:10.3791/56095

Keywords: Medicine, Issue 126, Chronic obstructive pulmonary disease, chronic bronchitis, emphysema, airflow limitation, lung parenchymal destruction, ozone exposure

Date Published: 8/25/2017

Citation: Sun, Z., Li, F., Zhou, X., Wang, W. Generation of a Chronic Obstructive Pulmonary Disease Model in Mice by Repeated Ozone Exposure. *J. Vis. Exp.* (126), e56095, doi:10.3791/56095 (2017).

Abstract

Chronic obstructive pulmonary disease (COPD) is characterized by persistent airflow limitation and lung parenchymal destruction. It has a very high incidence in aging populations. The current conventional therapies for COPD focus mainly on symptom-modifying drugs; thus, the development of new therapies is urgently needed. Qualified animal models of COPD could help to characterize the underlying mechanisms and can be used for new drug screening. Current COPD models, such as lipopolysaccharide (LPS) or the porcine pancreatic elastase (PPE)-induced emphysema model, generate COPD-like lesions in the lungs and airways but do not otherwise resemble the pathogenesis of human COPD. A cigarette smoke (CS)-induced model remains one of the most popular because it not only simulates COPD-like lesions in the respiratory system, but it is also based on one of the main hazardous materials that causes COPD in humans. However, the time-consuming and labor-intensive aspects of the CS-induced model dramatically limit its application in new drug screening. In this study, we successfully generated a new COPD model by exposing mice to high levels of ozone. This model demonstrated the following: 1) decreased forced expiratory volume 25, 50, and 75/ forced vital capacity (FEV_{25}/FVC, FEV_{50}/FVC, and FEV_{75}/FVC), indicating the deterioration of lung function; 2) enlarged lung alveoli, with lung parenchymal destruction; 3) reduced fatigue time and distance; and 4) increased inflammation. Taken together, these data demonstrate that the ozone exposure (OE) model is a reliable animal model that is similar to humans because ozone overexposure is one of the etiological factors of COPD. Additionally, it only took 6 - 8 weeks, based on our previous work, to create an OE model, whereas it requires 3 - 12 months to induce the cigarette smoke model, indicating that the OE model might be a good choice for COPD research.

Video Link

The video component of this article can be found at https://www.jove.com/video/56095/

Introduction

It has been estimated that COPD, including emphysema and chronic bronchitis, might be the third leading cause of death in the world in 2020[1,2]. The potential incidence of COPD in a population over 40 years old is estimated to be 12.7% in males and 8.3% in females within the next 40 years[3]. No medications are currently available to reverse the progressive deterioration in COPD patients[4]. Reliable animal models of COPD not only demand the imitation of the disease pathological process but also require a short generation period. Current COPD models, including the LPS or a PPE-induced model, can induce emphysema-like symptoms[5,6]. A single administration or a week-long challenge of LPS or PPE to mice or rats results in marked neutrophilia in the bronchoalveolar lavage fluid (BALF), increases pro-inflammatory mediators (*e.g.,* TNF-α and IL-1β) in the BALF or serum, produces lung parenchymal destruction-enlarged air spaces, and limits airflow[5,6,7,8,9,10]. However, LPS or PPE are not causes of human COPD and thus do not mimic the pathological process[11]. A CS-induced model produced a persistent airflow limitation, lung parenchymal destruction, and reduced functional exercise capacity. However, a traditional CS protocol requires at least 3 months to generate a COPD model[12,13,14,15]. Thus, it is important to generate a new, more efficient animal model that meets the two requirements.

Recently, in addition to cigarette smoking, air pollution and occupational exposure have become more common causes of COPD[16,17,18]. Ozone, as one of the major pollutants (though not the major component of air pollution), can directly react with the respiratory tract and damage the lung tissue of both children and young adults[19,20,21,22,23,24,25]. Ozone, as well as other stimulators including LPS, PPE, and CS, are involved in a serious of biochemical pathways of pulmonary oxidative stress and DNA damage and are linked to the initiation and promotion of COPD[26,27]. Another factor is that the symptoms of some COPD patients deteriorate after being exposed to ozone, indicating that ozone can disrupt lung function[18,28,29]. Therefore, we generated a new COPD model by repeatedly exposing mice to high concentrations of ozone for 7 weeks; this resulted in airflow defects and lung parenchymal damage similar to those of previous investigations[30,31,32]. We extended the OE protocol to female mice in this study and successfully reproduced the emphysema observed in male mice in our previous studies[30,31,32]. Because COPD mortality has decreased in men but increased in women in many countries[33], a COPD model in females is needed to study the mechanisms and

to develop therapeutic methods for female COPD patients. The applicability of the OE model to all genders lends further support to its use as a COPD model.

Protocol

NOTE: The OE model has been generated and used in previously reported research[30,31,32]. All animal experiments were approved by the Institutional Animal Care and Use Committee (IACUC) of Shanghai Jiaotong University.

1. Mice

1. House pathogen-free, 7- to 9-week-old female BALB/c mice in individual ventilated cages in an animal facility under controlled temperature (20 °C) and humidity (40 - 60%). Provide a 12 h light and 12 h dark cycle in the facility. Provide food and water *ad libitum*.

2. Ozone or Air Exposure

1. Generate ozone with an electric generator in a sealing acrylic (*e.g.* Perspex) box. Blow the air out of the box using a small air blower through an air vent pipe that is connected on the inside and outside of the box. Monitor the concentration of ozone in the box using an ozone probe. Wait until the concentration of ozone in the box reaches 2.5 parts per million (ppm).
   NOTE: The ozone probe can automatically switch the ozone generator on or off and can maintain the ozone level in the box at 2.5 ppm.
2. Place the mice into the box when the level of ozone reaches 2.5 ppm. Keep the mice in the box for 3 h each time to expose them to ozone.
   NOTE: The box can maintain an ozone level of 2.5 ppm during the 3 h by automatically switching the ozone generator on or off and blowing the CO_2 that is produced by the mice out of the box.
3. Give two ozone exposures (each exposure lasting 3 h) per week (once every 3 days) for 7 weeks; expose the control mice to air at the same time and for the same period.

3. Micro-computed Tomography

1. At the end of week 7, anesthetize the mice with an intraperitoneal injection of pelltobarbitalum natricum (1%, 0.6 - 0.8 ml/100 g) adjust the dose according to individual situations to see that the mouse does not respond to a toe pinch. Monitor and keep the mouse at a steady breathing frequency; and make sure no voluntary motions exist during the procedures.
2. Place the anesthetized mice in the chamber of a micro-computed tomography (μCT).
3. Calibrate the μCT using the standard protocol and the manufacturer's instructions. Set the X-ray tube at 50 kV and the current at 450 μA.
   NOTE: Both the X-ray and the detector rotate around the mice.
4. Perform the μCT analysis by acquiring 515 projections with an effective pixel size of 0.092 mm, an exposure time of 300 ms for one slice, and a slice thickness of 0.093 mm.
5. Reconstruct the lung with the acquired images using a software. Adjust the grayscale image brightness by setting the minimum and maximum of the grayscale at -750 and -550 Hounsfield units, respectively.
   NOTE: The software will automatically calculate the volumes of the lung parenchyma and the low-attenuation area (LAA)[34,35].
6. Calculate the percentage of LAA (LAA%) by dividing the LAA volume by the total lung volume.

4. Treadmill Test

1. Give the mice an adaptation test at a speed of 10 m/min for 10 min on a running treadmill machine. Note: The electricity is always off when the procedure is being conducted.
2. Administer a fatigue test to the mice.
   1. Warm up the mice at a speed of 10 m/min for 5 min.
   2. Increase the speed to 15 m/min for 10 min.
   3. Increase the exercise intensity: increasing the speed by 5 m/min, starting at 20 m/min, every 30 min until mice cannot continue to run[36].
3. Record the total running distance and running time as fatigue distance and fatigue time, respectively.

5. Pulmonary Function Measurements

1. Anesthetize the mice with an intraperitoneal injection of pelltobarbitalum natricum (1%, 0.6 - 0.8 ml/100 g) adjust the dose according to individual situations to see that the mouse does not respond to a toe pinch and wait until the mice have maintained spontaneous breathing. Monitor and keep the mouse at a steady breathing frequency; and make sure no voluntary motions exist during the procedures.
2. Carefully tracheostomize the mice and place them in a body plethysmograph that is connected to a computer-controlled ventilator.
   NOTE: Ventilation is controlled via a valve located proximally to the endotracheal tube. The setup provides different semi-automatic maneuvers, including the maneuver of the quasi-static pressure volume and the maneuver of the fast flow volume.
3. Impose an average breathing frequency of 150 breaths/min to the anesthetized mouse via pressure-controlled ventilation until a regular breathing pattern and complete expiration at each breathing cycle is obtained.
4. Perform the quasi-static pressure-volume maneuver with the device by using the negative pressures generated in the plethysmograph.
5. Perform the fast flow volume maneuver within the quasi-static pressure-volume loops to record the FVC and the FEV. Inflate the lung to +30 cm H_2O and immediately afterwards connect it to a highly negative pressure to enforce expiration until the residual volume is at -30 cm H_2O.

Record the FEV in the first 25, 50, and 75 ms of exhalation (FEV_{25}, FEV_{50}, and FEV_{75}, respectively). Reject the suboptimal maneuvers. For each test with every single mouse, conduct a minimum of three acceptable maneuvers to obtain a reliable mean for all numerical parameters.

6. BALF Collection

1. Following terminal anesthesia with pelltobarbitalum natricum ((1%, 1.8-2.4 ml/100 g) adjust the dose according to individual situations to see that the mouse does not respond to a toe pinch and lose breath), lavage the mice with 2 mL of PBS via a 1 mm-diameter endotracheal tube and then retrieve the BALF[10].
2. Pool the retrieved lavage aliquots and centrifuge them at 4 °C and 250 x g for 10 min.
3. Collect the supernatant for immediate use and store the remainder at -80 °C or liquid nitrogen.
4. Count the total number of cells using a hemocytometer.
5. Resuspend the cell pellet in PBS and then spin (1,400 x g, 6 min) 250 µL of resuspended cells onto slides using a slide spinner centrifuge.
6. Apply Wright staining to cells on the slides according to the manufacturer's protocol.
7. Count 200 cells per mouse; identify the cells as macrophages or neutrophils, according to standard morphology, under 400X magnification; and count their numbers.

7. Cardiac Blood Sampling

1. Collect blood via cardiac puncture, load it into 1.5-mL tubes, and keep it on ice for 30 min.
2. Centrifuge the blood samples for 5 min at 2,000 x g and 4 °C.
3. Transfer the supernatant (serum) to a new tube and store it at -80 °C or liquid nitrogen.
4. Prepare the serum for IL-1β, IL-10, and TNF-α detection tests using the respective ELISA kits.

8. Lung Morphometric Analysis

1. Dissect the lungs and tracheas from the mice.
    1. Position each euthanized mouse onto a surgical board immediately after sacrifice.
    2. Dissect away the platysma and anterior tracheal muscles to visualize and access the tracheal rings.
    3. Open up the thoracic cavity. Dissect the lungs and the trachea, but do not separate the heart from the lungs.
2. Connect the endotracheal catheter to a syringe containing 4% paraformaldehyde through a PE90 polyethylene tube.
   Caution: Paraformaldehyde is toxic. Wear gloves and safety glasses and use the solution inside a fume hood.
3. Inflate the lung completely using 4% paraformaldehyde (10 drops, ~200 µL) through the endotracheal catheter. Remove the heart after the completion of inflation.
4. Maintain the lung in a 15 mL tube containing 10 mL of 4% paraformaldehyde for at least 4 h.
5. Embed the lung in paraffin. Obtain 5-µm sections by paraffin block sectioning with a rotary microtome. During the sectioning, expose the maximum surface area of lung tissue within the bronchial tree area.
6. For morphometric analysis, perform hematoxylin and eosin (H&E) staining on the sections.
7. Image the sections with a bright-field upright microscope (objective lens, 20X; exposure time, 1.667 ms).
8. Have two investigators blinded to the treatment protocol independently count the histological sections. Use the mean linear intercept (L_m) as a parameter for measuring the distance of the inter-alveolar septal wall. Determine the L_m using the following steps:
    1. Open the images of the sections in Photoshop and draw a reticule-grid on the image with five 550 µm long lines.
    2. Count the number of alveoli across the grid line.
    3. Calculate the L_m by dividing the length of the grid line by the number of alveoli. For quantification, image five sections per mouse. Acquire ten images of each section (one image per field) and assess randomly. During field selection, avoid fields of airways and vessels by moving one field ahead or in another direction.
       Note: The data are presented as the mean ± S.E.M. An un-paired t-test was carried out for comparison between air-exposed mice and ozone-exposed mice. Three animals of each group were used to calculate the significant difference. A p-value of <0.05 was considered significant.

Representative Results

Examples of 3D µCT images of each group are displayed in **Figure 1a**. The ozone-exposed mice had a significantly larger total lung volume (**Figure 1a and b**) and LAA% (**Figure 1c**) than did the air-exposed control mice. The lung volume and LAA% remained elevated after six weeks of ozone exposure[31,32]. Increased lung volume and LAA% represent the emphysema phenotype. Examples of lung alveolar enlargement in **Figure 2a** illustrate the emphysema formation. An increase in the mean linear intercept (Lm) was observed in ozone-exposed mice (**Figure 2b**), which confirmed that lung parenchymal destruction occurred after ozone exposure.

Lung function was measured by the airflow rate parameters, shown as FEV_{25}/FVC, FEV_{50}/FVC, and FEV_{75}/FVC. The results showed that all of the parameters that decreased in ozone-exposed mice (**Figure 3a-c**) were consistent with the typical lung functional defects in COPD patients[4,37]. To further evaluate the OE model, we carried out an exercise tolerance test that substituted for the 6-min walk test (6MWT)[38,39], which is commonly used to assess changes in functional exercise capacity in COPD patients. The ozone exposure significantly decreased the fatigue time and fatigue distance (**Figure 4a and b**).

To address the pathogenesis of COPD in the OE model, the macrophages and neutrophils were counted from the BALFs of the mice; pro-inflammatory cytokines (IL-1β and TNF-α) and anti-inflammatory cytokines (IL-10) were detected in the mouse sera. The ozone-exposed mice showed a significant increase in inflammatory cells, including macrophages and neutrophils (**Figure 5a-c**), as well as a significant decrease in IL-10 and an increase in IL-1β and TNF-α (**Figure 6a-c**). All of the data demonstrated that the OE model recapitulated human COPD-like symptoms.

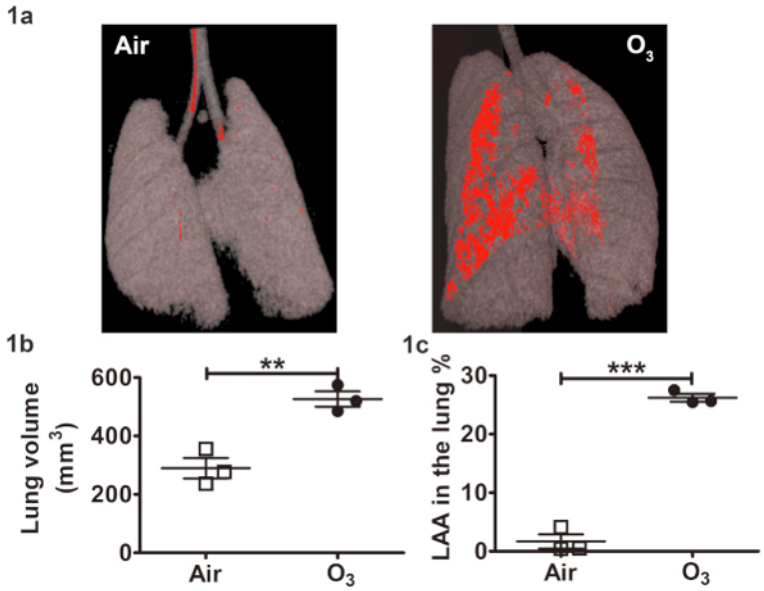

Figure 1.**Ozone exposure increased the lung volume and LAA% detected by μCT.**(a) Representative 3D images showing the lungs of air- or ozone-exposed mice at 7 weeks after the respective exposure. (b) Individual total lung volumes of the two groups were extracted from the 3D images for statistics. Ozone-exposed mice showed a significant increase in total lung volume. (c) Individual and mean LAA% of the two groups. Ozone-exposed mice showed a significant increase in LAA%. The red color indicates LAA (voxels with densities of 2,550-2,700 Hounsfield units). The trachea and bronchi shown in red in this figure were removed to calculate the lung LAA. The data are presented as the mean ± S.E.M. **P<0.01, ***P<0.001. Please click here to view a larger version of this figure.

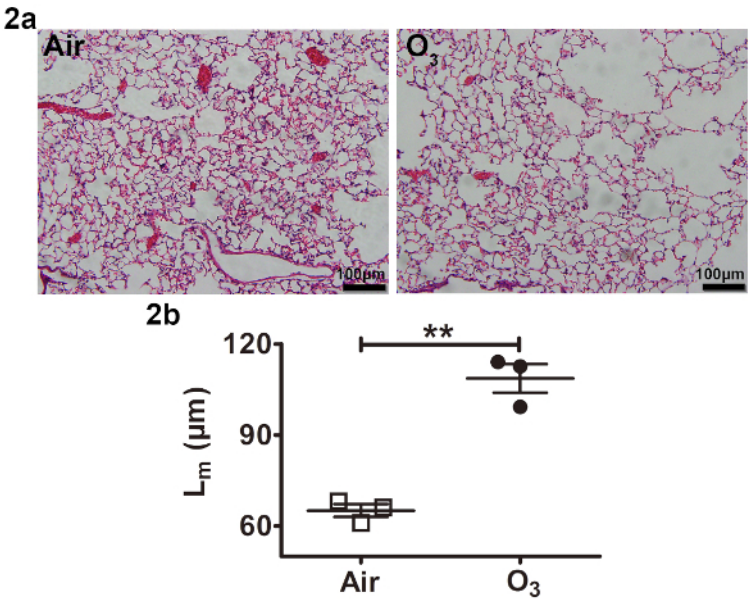

Figure 2. **Ozone exposure increased the Lm.** (a) Representative micrographs of lung alveolar spaces in HE-stained sections of air-exposed or ozone-exposed mice. (b) Individual values of Lm were quantified from the lung sections of the two groups for statistics. An increase in Lm was observed in ozone-exposed mice. The data are presented as the mean ± S.E.M. **P<0.01. Please click here to view a larger version of this figure.

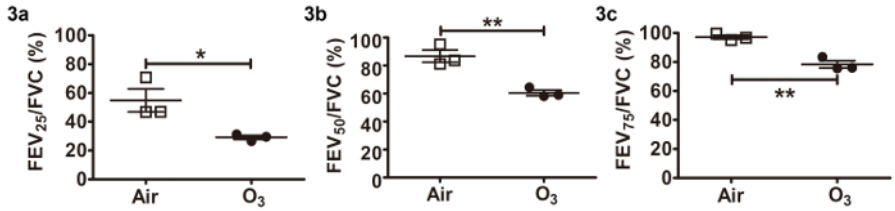

Figure 3. Ozone exposure decreased pulmonary function. (a-c) For both the air-exposed and the ozone-exposed mice, the individual FEV in the first 25, 50, and 75 ms of fast expiration (FEV_{25}, FEV_{50}, and FEV_{75}, respectively), as well as the FVC, were all recorded. The percentages of FEV_{25}, FEV_{50}, and FEV_{75} to FVC were calculated separately. FEV_{25}/FVC, FEV_{50}/FVC, and FEV_{75}/FVC all decreased significantly in ozone-exposed mice. The data are presented as the mean ± S.E.M. *P<0.05, **P<0.01. Please click here to view a larger version of this figure.

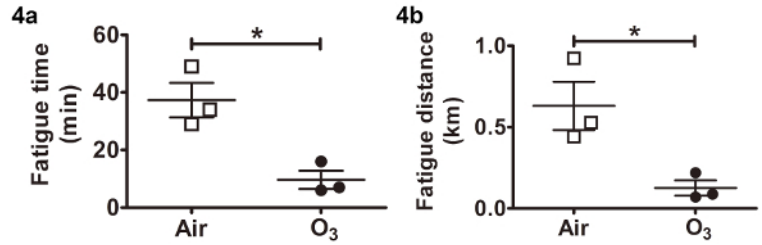

Figure 4. Ozone exposure decreased fatigue time and fatigue distance. (a) Individual running times for air- or ozone-exposed mice were recorded. Ozone-exposed mice showed a significant decrease in fatigue time. (b) Individual running distances of the two groups were recorded. Ozone-exposed mice exhibited a significant decrease in fatigue distance. The data are presented as the mean ± S.E.M. *P<0.05. Please click here to view a larger version of this figure.

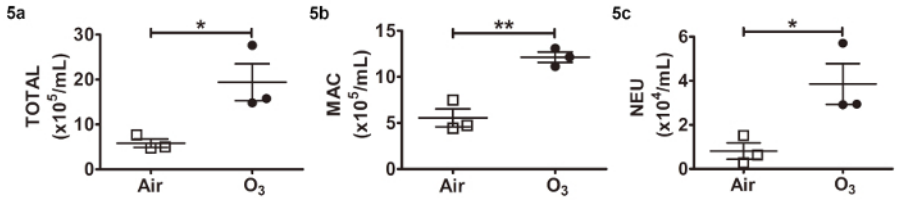

Figure 5. Inflammatory cells counted from BALF. (a) Individual and mean numbers of total cells (TOTAL) in air- or ozone-exposed mice. (b) Individual and mean numbers of macrophages (MAC) in the two groups. (c) Individual and mean numbers of neutrophils (NEU) in the two groups. The data are presented as the mean ± S.E.M. *P<0.05, **P<0.01. Please click here to view a larger version of this figure.

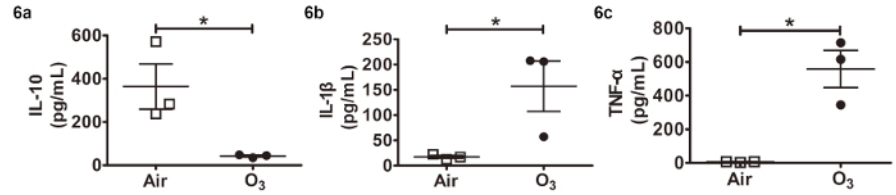

Figure 6. Inflammatory and anti-inflammatory cytokine detection in serum. (a) Individual and mean values of the amount of IL-10 in air- or ozone-exposed mice. (b) Individual and mean values of the amount of IL-1β in the two groups. (c) Individual and mean values of the amount of TNF-α in the two groups. The data are presented as the mean ± S.E.M. *P<0.05. Please click here to view a larger version of this figure.

Discussion

In this study, we present a reliable method for generating a new COPD model. Compared to other models (*i.e.,* LPS or PPE models), this OE model recapitulates the pathological process of COPD patients. Because cigarette smoke is the main hazardous material that causes COPD in human patients[40], the CS model remains the most popular COPD model[41,42]. However, the CS model requires a 3- to 12-month R&D period for new drugs. Compared to the CS model, the current OE model reduces the generation period to 6-8 weeks. We have observed emphysema in male mice after 6 weeks of exposure to ozone in our previous studies[30,31,32]. In this study, we applied the OE protocol to female mice for 7 weeks and successfully generated a female OE model. Because it has been reported that COPD mortality has decreased in men but increased in women in some countries[33], it is necessary to study the pathogenic mechanisms and to develop cure approaches for female COPD patients using a female COPD model. We know that the abovementioned COPD models (*i.e.,* LPS, PPE, and CS) can work in both male and female animals[43]. The aim of this work was to propose an additional COPD model that both recapitulates the pathological process of COPD patients and requires a very short generation-period.

The key step for generating this model was exposing the mice to ozone (at a level of 2.5 ppm) two times per week (once every 3 days) for 6-8 weeks (in this study, we used 7 weeks, although we did not try dose escalation). By controlling the critical parameters of exposure frequency and ozone concentration, we successfully reproduced emphysema in male C57BL/6 mice[31,32], male BALB/c mice[30], and female BALB/c mice (the

current study). The emphysema phenotype resulted from ozone exposure, with the airflow limitation and lung parenchymal destruction similar to the changes seen in COPD patients[44,45].

There are still limitations to this study. For example, because the pathogenesis of human COPD is related to the anatomy of the lungs, an ideal COPD model should be generated in animals that have a pulmonary anatomical structure similar to that of humans.Compared to large animals, small animals possess even less extensive airway branching than humans[46]. We must admit that it would be more meaningful to generate a COPD model in large animals. However, it is very difficult to establish large-scale models in animals. Another limitation of this model is its clinical relevance. Although it is certain that ozone can react with the respiratory tract and damage lung tissue[19,22], and although there is evidence that the symptoms of some COPD patients deteriorate after exposure to ozone[28], ozone is not the main cause of COPD in patients. However, we are still proposing and using this OE model because both ozone and CS cause damage to the respiratory system by inducing inflammation and lead to oxidative stress[26,27]. Thus, a new drug that can cure COPD in the OE model can assumably also work in the CS model and therefore potentially be developed for COPD patients.

Applications of the OE model are not restricted to deciphering the molecular and cellular mechanisms of COPD. Our two recent papers also investigated the efficacy of N-acetylcysteine (NAC)[31] and NaHS[32] (an exogenous donor of H_2S) at treating COPD via the exogenous administration of the two drugs to the OE model. In the first study, we found a reversal of airway hyper-responsiveness and a reduction of airway smooth muscle mass after the administration of NAC. These effects might indicate the basis for potential clinical benefits of NAC in COPD patients[31]. In the second study of the OE model, we found that the administration of exogenous NaHS reversed lung inflammation and partially reversed the features of emphysema. Thus, with this OE model, we demonstrated in a preliminary study that NaHS could be developed as a potential drug candidate for COPD patients[32]. Therefore, the OE model has potential applications for both mechanism research and drug screening for COPD.

Disclosures

Z.W.S. and W.W. are current employees and stock option holders of the Cellular Biomedicine Group (NASDAQ: CBMG). The other authors declare that they have no competing interests.

Acknowledgements

The authors would like to express gratitude to Mr. Boyin Qin (Shanghai Public Health Clinical Center) for the technical assistance with the μCT evaluation in this protocol.

References

1. Lozano, R. *et al.* Global and regional mortality from 235 causes of death for 20 age groups in 1990 and 2010: a systematic analysis for the Global Burden of Disease Study 2010. *Lancet.* **380**, 2095-2128 (2012).
2. Chapman, K. R. *et al.* Epidemiology and costs of chronic obstructive pulmonary disease. *Eur Respir J.* **27**, 188-207 (2006).
3. Afonso, A. S., Verhamme, K. M., Sturkenboom, M. C., Brusselle, G. G. COPD in the general population: prevalence, incidence and survival. *Respir Med.* **105**, 1872-1884 (2011).
4. Rabe, K. F. *et al.* Global strategy for the diagnosis, management, and prevention of chronic obstructive pulmonary disease: GOLD executive summary. *Am J Respir Crit Care Med.* **176**, 532-555 (2007).
5. Ogata-Suetsugu, S. *et al.* Amphiregulin suppresses epithelial cell apoptosis in lipopolysaccharide-induced lung injury in mice. *Biochem Biophys Res Communi.* **484**, 422-428 (2017).
6. Oliveira, M. V. *et al.* Characterization of a Mouse Model of Emphysema Induced by Multiple Instillations of Low-Dose Elastase. *Front Physiol.* **7**, 457 (2016).
7. Vernooy, J. H., Dentener, M. A., van Suylen, R. J., Buurman, W. A., Wouters, E. F. Long-term intratracheal lipopolysaccharide exposure in mice results in chronic lung inflammation and persistent pathology. *Am J Respir Cell Mol Biol.* **26**, 152-159 (2002).
8. Birrell, M. A. *et al.* Role of matrix metalloproteinases in the inflammatory response in human airway cell-based assays and in rodent models of airway disease. *J Pharm Exp Ther.* **318**, 741-750 (2006).
9. Gamze, K. *et al.* Effect of bosentan on the production of proinflammatory cytokines in a rat model of emphysema. *Exp Mol Med.* **39**, 614-620 (2007).
10. Vanoirbeek, J. A. *et al.* Noninvasive and invasive pulmonary function in mouse models of obstructive and restrictive respiratory diseases. *Am J Respir Cell Mol Biol.* **42**, 96-104 (2010).
11. Wright, J. L., Cosio, M., Churg, A. Animal models of chronic obstructive pulmonary disease. *Am J Physiol Lung Cell Mol Physiol.* **295**, L1-15 (2008).
12. Huh, J. W. *et al.* Bone marrow cells repair cigarette smoke-induced emphysema in rats. *Am J Physiol Lung Cell Mol Physiol.* **301**, L255-266 (2011).
13. Schweitzer, K. S. *et al.* Adipose stem cell treatment in mice attenuates lung and systemic injury induced by cigarette smoking. *Am J Respir Crit Care Med.* **183**, 215-225 (2011).
14. Guan, X. J. *et al.* Mesenchymal stem cells protect cigarette smoke-damaged lung and pulmonary function partly via VEGF-VEGF receptors. *J Cell Biochem.* **114**, 323-335 (2013).
15. Gu, W. *et al.* Mesenchymal stem cells alleviate airway inflammation and emphysema in COPD through down-regulation of cyclooxygenase-2 via p38 and ERK MAPK pathways. *Sci Rep.* **5**, 8733 (2015).
16. Cordasco, E. M., & VanOrdstrand, H. S. Air pollution and COPD. *Postgrad Med.* **62**, 124-127 (1977).
17. Berend, N. Contribution of air pollution to COPD and small airway dysfunction. *Respirology.* **21**, 237-244 (2016).
18. DeVries, R., Kriebel, D., Sama, S. Outdoor Air Pollution and COPD-Related Emergency Department Visits, Hospital Admissions, and Mortality: A Meta-Analysis. *COPD.* **14** (1), 113-121 (2016).

19. Penha, P. D., Amaral, L., Werthamer, S. Ozone air pollutants and lung damage. *IMS Ind Med Surg.* **41**, 17-20 (1972).
20. Stern, B. R. *et al.* Air pollution and childhood respiratory health: exposure to sulfate and ozone in 10 Canadian rural communities. *Environ Res.* **66**, 125-142 (1994).
21. Tager, I. B. *et al.* Chronic exposure to ambient ozone and lung function in young adults. *Epidemiology.* **16**, 751-759 (2005).
22. Romieu, I., Castro-Giner, F., Kunzli, N., Sunyer, J. Air pollution, oxidative stress and dietary supplementation: a review. *Eur Respir J.* **31**, 179-197 (2008).
23. Hemming, J. M. *et al.* Environmental Pollutant Ozone Causes Damage to Lung Surfactant Protein B (SP-B). *Biochemistry.* **54**, 5185-5197 (2015).
24. Chu, H. *et al.* Comparison of lung damage in mice exposed to black carbon particles and ozone-oxidized black carbon particles. *Sci Total Environ.* **573**, 303-312 (2016).
25. Jin, M. *et al.* MAP4K4 deficiency in CD4(+) T cells aggravates lung damage induced by ozone-oxidized black carbon particles. *Environ Toxicol Pharmacol.* **46**, 246-254 (2016).
26. Brusselle, G. G., Joos, G. F., Bracke, K. R. New insights into the immunology of chronic obstructive pulmonary disease. *Lancet.* **378**, 1015-1026 (2011).
27. Valavanidis, A., Vlachogianni, T., Fiotakis, K., Loridas, S. Pulmonary oxidative stress, inflammation and cancer: respirable particulate matter, fibrous dusts and ozone as major causes of lung carcinogenesis through reactive oxygen species mechanisms. *Int J Environ Res Public Health.* **10**, 3886-3907 (2013).
28. Medina-Ramon, M., Zanobetti, A., Schwartz, J. The effect of ozone and PM10 on hospital admissions for pneumonia and chronic obstructive pulmonary disease: a national multicity study. *Am J Epidemiol.* **163**, 579-588 (2006).
29. Lee, I. M., Tsai, S. S., Chang, C. C., Ho, C. K., Yang, C. Y. Air pollution and hospital admissions for chronic obstructive pulmonary disease in a tropical city: Kaohsiung, Taiwan. *Inha Toxicol.* **19**, 393-398 (2007).
30. Triantaphyllopoulos, K. *et al.* A model of chronic inflammation and pulmonary emphysema after multiple ozone exposures in mice. *Am J Physiol Lung Cell Mol Physiol.* **300**, L691-700 (2011).
31. Li, F. *et al.* Effects of N-acetylcysteine in ozone-induced chronic obstructive pulmonary disease model. *PLoS ONE.* **8**, e80782 (2013).
32. Li, F. *et al.* Hydrogen Sulfide Prevents and Partially Reverses Ozone-Induced Features of Lung Inflammation and Emphysema in Mice. *Am J Respir Cell Mol Biol.* **55**, 72-81 (2016).
33. Rycroft, C. E., Heyes, A., Lanza, L., Becker, K. Epidemiology of chronic obstructive pulmonary disease: a literature review. *Int J Chron Obstruct Pulmon Dis.* **7**, 457-494 (2012).
34. Washko, G. R. *et al.* Airway wall attenuation: a biomarker of airway disease in subjects with COPD. *J Appl Physiol.* **107**, 185-191 (2009).
35. Yamashiro, T. *et al.* Quantitative assessment of bronchial wall attenuation with thin-section CT: An indicator of airflow limitation in chronic obstructive pulmonary disease. *AJR Am J Roentgenol.* **195**, 363-369 (2010).
36. Tang, X. *et al.* Arctigenin efficiently enhanced sedentary mice treadmill endurance. *PLoS ONE.* **6**, e24224 (2011).
37. Schmidt, G. A. *et al.* Official Executive Summary of an American Thoracic Society/American College of Chest Physicians Clinical Practice Guideline: Liberation from Mechanical Ventilation in Critically Ill Adults. *Am J Respir Crit Care Med.* **195**, 115-119 (2017).
38. ATS Committee on Proficiency Standards for Clinical Pulmonary Function Laboratories. ATS statement: guidelines for the six-minute walk test. *Am J Respir Crit Care Med.* **166**, 111-117 (2002).
39. Shigemura, N. *et al.* Autologous transplantation of adipose tissue-derived stromal cells ameliorates pulmonary emphysema. *Am J Transplant.* **6**, 2592-2600 (2006).
40. Bchir, S. *et al.* Concomitant elevations of MMP-9, NGAL, proMMP-9/NGAL and neutrophil elastase in serum of smokers with chronic obstructive pulmonary disease. *J Cell Mol Med.* 1-12 (2016).
41. Fricker, M., Deane, A., Hansbro, P. M. Animal models of chronic obstructive pulmonary disease. *Expert Opin Drug Discov.* **9**, 629-645 (2014).
42. Perez-Rial, S., Giron-Martinez, A., Peces-Barba, G. Animal models of chronic obstructive pulmonary disease. *Arch Bronconeumol.* **51**, 121-127 (2015).
43. Antunes, M. A. *et al.* Effects of different mesenchymal stromal cell sources and delivery routes in experimental emphysema. *Respir Res.* **15**, 118 (2014).
44. Celli, B. R., MacNee, W., Force, A. E. T. Standards for the diagnosis and treatment of patients with COPD: a summary of the ATS/ERS position paper. *Eur Respir J.* **23**, 932-946 (2004).
45. U.S. Preventive Services Task Force. Screening for chronic obstructive pulmonary disease using spirometry: U.S. Preventive Services Task Force recommendation statement. *Ann Intern Med.* **148**, 529-534 (2008).
46. Ward, R. E. *et al.* Design considerations of CareWindows, a Windows 3.0-based graphical front end to a Medical Information Management System using a pass-through-requester architecture. *Proc Annu Symp Comput Appl Med Care.* 564-568 (1991).

